geomatics

MDPI

Article

SLAM Mobile Mapping for Complex Archaeological Environments: Integrated Above–Below-Ground Surveying

Gabriele Bitelli, Anna Forte * and Emanuele Mandanici

Department of Civil, Chemical, Environmental and Materials Engineering (DICAM), University of Bologna, Viale del Risorgimento 2, 40136 Bologna, Italy; gabriele.bitelli@unibo.it (G.B.); emanuele.mandanici@unibo.it (E.M.)
* Correspondence: anna.forte3@unibo.it

Abstract

Archaeological sites characterized by the coexistence of extensive above-ground terrain and hypogeum structures present major challenges for accurate and comprehensive geospatial documentation. Conventional survey approaches—such as static terrestrial laser scanning (TLS), total-station measurements, and aerial photogrammetry—often suffer from operational constraints, particularly in the presence of narrow underground spaces, low or absent illumination, harsh environmental conditions, and restrictions on UAV deployment. Additional complexity arises when both surface and subterranean elements must be consistently georeferenced to a common global reference system, especially where establishing a traditional topographic–geodetic control network is impractical. Within the framework of the EIMAWA Egyptian–Italian Mission conducted by the University of Milano since 2018, the Geomatics group of the University of Bologna designed and implemented a multi-scale multi-technique 3D documentation workflow, with a prominent role assumed by Simultaneous Localization and Mapping (SLAM) mobile laser scanning. The approach was supported by GNSS measurements providing centimetric accuracy. SLAM was employed to document both the surface necropolis and multiple hypogeal tombs, enabling rapid acquisition of dense three-dimensional data in environments where traditional techniques are limited. All datasets were integrated within a unified reference system, resulting in a coherent, multi-layered spatial dataset representing both landscape and underground spaces. The results demonstrate that SLAM can produce dense point clouds that document at few-centimetric level accuracy and continuously both above- and below-ground contexts. Quantitative analyses of the co-registration and mutual alignment of multiple SLAM datasets confirm a high degree of internal consistency, further enhanced through post-processing refinement. Overall, the experience indicates that this solution represents a practical and reliable technique for complex archaeological surveying.

Keywords: SLAM; mobile laser scanning; archaeological survey; hypogeal structures; GNSS georeferencing; cultural heritage

Academic Editors: Efstratios Stylianidis and Gino Dardanelli

Received: 13 February 2026
Revised: 16 March 2026
Accepted: 22 March 2026
Published: 26 March 2026

1. Introduction

The documentation of archaeological and cultural heritage sites increasingly leverages geomatic techniques to produce accurate, georeferenced, multi-scale three-dimensional reconstructions. Contemporary practice favours integrated workflows combining active and passive sensors to capture large, complex sites across multiple spatial scales. Terrestrial laser scanning (TLS), terrestrial photogrammetry and unmanned aerial vehicle (UAV)

photogrammetry have proven particularly effective in generating dense, metrically reliable point clouds across varied scales, morphologies and acquisition conditions [1–5].

Traditional techniques from the geomatic domain can be employed effectively for complex morphology scenarios and for integrated above–below-ground surveying, though with certain challenges that have been discussed in the related literature. For instance, Ebolese et al. [6] demonstrate this in their comprehensive survey of the Sybil hypogeum and associated superstructure at Lilibeo (Italy), where the fusion of terrestrial range data and UAV imagery yielded a unified model capable of representing both underground spaces and open-air contexts with geometric accuracy. This study highlights the value of sensor integration in addressing the heterogeneous demands of hypogeal environments. Similarly, Aricò et al. [7] present integrated TLS and photogrammetric methodologies for documenting the Roman hypogeum of Crispia Salvia, showing that photogrammetry provides detailed surface texture while TLS ensures geometric completeness even in occluded subterranean chambers. Such multiscale approaches are indispensable where access constraints, poor lighting, and structural complexity pose challenges to single-technique surveys.

For extended archaeological landscapes, the multi-temporal integration of geomatic products enables diachronic analysis and monitoring: Chiabrando et al. [8] illustrate this through long-term datasets at Hierapolis, demonstrating how historical imagery, UAV photogrammetry, and airborne LiDAR can be integrated to create evolving three-dimensional records of expansive archaeological terrains. Beyond archaeological landscapes, applications at the Al Ula monumental tombs complex confirm that high-resolution TLS combined with UAV photogrammetry can document complex structures and their surrounding topography with high geometric detail, supporting both conservation and interpretation strategies [9].

Despite their maturity and consolidated effectiveness, such approaches remain challenged by contexts that combine large surface extents with subterranean structures. In these environments, limited accessibility, poor illumination, rugged terrain and restrictions on UAV deployment may significantly increase acquisition time and reduce survey completeness. In recent years, Simultaneous Localisation And Mapping (SLAM), particularly mobile LiDAR- and Vision-based systems, has emerged as a promising alternative for documenting both open and enclosed, morphologically complex environments [10,11]. Unlike static TLS, SLAM-based mobile mapping enables continuous 3D geospatial data acquisition as the operator traverses the site, producing dense point clouds that can cover extensive areas or intricate interiors in a comparatively short time. Real-time estimation of the sensor trajectory is based on redundant geometric constraints derived from overlapping observations, combined with iterative matching of geometric or visual features between successive scans, thereby enabling dynamic point clouds' registration through global least-square adjustment and sensor fusion (typically LiDAR and inertial measurements) during motion [12]. Its operational flexibility, combined with relatively accessible hardware costs and increasing algorithmic robustness, is expanding SLAM uptake in archaeology and heritage documentation [13,14], and different solutions have been recently proposed and tested—through comparison with static acquisition devices—to optimise the data acquisition with such instruments [15–17].

Significant examples of the SLAM use for complex archaeological scenarios—which, as mentioned, can pose challenges to traditional methods—are found in the literature. An indoor mobile mapping system (iMMS) was applied to the rock-cut Hypogeum of Calaforno (Sicily), characterised by narrow passages, irregular morphology and limited lighting; comparison with TLS and photogrammetry showed that SLAM provides a viable and efficient alternative, particularly for complex underground heritage environments [18].

Similarly, the survey of Bossea Cave (Piedmont, Italy)—a karst system of both natural and anthropogenic interest—demonstrated that portable SLAM-based mapping can document both the above-ground mountain slope and the internal cave geometry. Validation against TLS revealed planimetric deviations up to approximately 15 cm and vertical deviations up to approximately 22 cm, highlighting both the method's potential and limitations [19].

More broadly, research on SLAM in extreme and subterranean environments demonstrates both the maturity and intrinsic difficulties of LiDAR-centric SLAM in tunnels, mines, and other GNSS-denied spaces and adverse sensing conditions, emphasising robust back-end loop-closure strategies and multi-robot or multi-sensor configurations [20]. Recently, mobile mapping has been integrated with photogrammetry and semantic segmentation in heritage contexts, for example, through the combination of visual SLAM (V-SLAM) with deep-learning–based semantic annotation to document and enrich architectural heritage datasets [21]. These studies confirm that mobile SLAM technology is no longer confined to robotics or civil engineering but is increasingly adopted in cultural heritage, archaeology and underground-structure documentation. Nonetheless, applications to large-scale archaeological sites combining surface topography and hypogeal structures remain rare in the literature.

Overall, in this field, the literature indicates an increasing interest in mobile and continuous mapping approaches with respect to static, station-based geomatic workflows. Traditional techniques such as TLS and UAV photogrammetry remain the reference standard for geometric accuracy, radiometric quality, and rigorous georeferencing, particularly in open or architecturally accessible contexts. However, their operational constraints become evident in complex archaeological environments characterised by narrow hypogea, multi-level structures, limited lighting, or restricted UAV use, where acquisition time and occlusions may compromise efficiency and completeness. Conversely, SLAM-based mobile mapping enables rapid, uninterrupted data acquisition across both surface and subterranean spaces, offering greater flexibility and spatial continuity in GNSS-denied and morphologically complex settings. Although SLAM-derived datasets currently exhibit lower absolute accuracy and susceptibility to drift, different studies [22,23] demonstrate that these limitations can be mitigated through loop-closure strategies and integration with external control. Consequently, SLAM should be viewed not as a replacement but as a complementary methodology that significantly extends the operational scope of three-dimensional archaeological documentation, particularly for extensive and complex landscapes integrating surface and hypogeal structures.

In this context, this paper documents and evaluates the use of SLAM mobile laser scanning in the framework of the EIMAWA (Egyptian–Italian Mission at West Aswan) archaeological mission (2018–present), with the aim of surveying a desert necropolis with both surface structures and subterranean tombs. The article describes the methodological workflow and its integration with GNSS measurements, analysing the potential and limitations of SLAM in such demanding archaeological contexts. From a methodological standpoint, the primary objective of this study is to demonstrate a SLAM-based workflow for rapid, georeferenced three-dimensional documentation in a complex excavation environment, with an emphasis on operational feasibility, descriptive completeness, and field efficiency. Accordingly, the aim is not to conduct a controlled benchmarking of the SLAM system's intrinsic positional accuracy, but rather to present the adopted methodology as a practical and operational solution for large and complex archaeological sites characterized by harsh environmental conditions and logistical constraints, within the framework of extensive 3D documentation activities.

2. Materials and Methods

2.1. Study Area and Archaeological Context: The EIMAWA Archaeological Mission at the Aga Khan Necropolis, Aswan

The surveyed site is a wide desert necropolis located on the west bank of the Nile River in Aswan, Egypt, near the Aga Khan mausoleum. This archaeological complex features a large number of hypogeum tombs, surface structures, and burial remains, covering an excavation area that—up to now—amounts to 25,000 square meters (though, the entire area of interest of the archaeological mission extends to more the 200,000 square meters). The necropolis, used between the late Pharaonic period (5th century BC) and the early Roman era (2nd–3rd century AD), preserves extensive evidence of long-term funerary practices and cultural interaction in the Aswan region [24]. The EIMAWA mission, promoted by the University of Milan and directed by Prof. P. Piacentini, has been studying the necropolis since 2018 with a multidisciplinary approach. EIMAWA, in fact, includes chemists, biologists, geologists, botanists, anthropologists, radiologists, and surveyors who work alongside Egyptologists to investigate the history, customs, and material culture of the populations that inhabited this area [25]. In addition to scientific analysis from several fields, the archaeological project also required an important surveying activity, not a simple one, given its extent and topographical complexity. The Geomatics team at the DICAM Department of the University of Bologna is in charge of these operations and has carried out several related activities, including the implementation of techniques such as high-resolution photogrammetry and satellite imagery processing, which are not described here as they fall outside the scope of the present article.

Environmental conditions are challenging: high temperatures, wind, sand, and dust, along with limited time windows for excavation. Furthermore, UAV deployment is not permitted, precluding the use of aerial photogrammetry for surface documentation. The combined complexity of large surface extent (combining both morphologically rich and highly flat and uniform areas, Figure 1), uneven terrain, and subterranean tombs with narrow corridors, chambers, and poor illumination made the site an ideal candidate for testing SLAM-based mobile mapping as a core documentation technique.

While an initial topographic field survey was conducted in 2019, most of the 3D data acquisition took place during two campaigns in May 2023 and May 2025.

Figure 1. A view of the desert landscape where the archaeological site is located.

2.2. Data Georeferencing

As mentioned above, one objective of the geomatic survey conducted during the archaeological mission was to model the site topography in 3D to analyse the morphology of the necropolis and the spatial distribution of the tombs across the area. A basic component of the developed methodology was the establishment of an absolute, high-accuracy geodetic reference system that could serve as a spatial constraint among different epochs of field acquisitions and as a basis for potential GIS-oriented applications. To this end, a reference GNSS antenna was installed on the roof of an electrical cabin located within the site (Figure 2). This master position was determined using the Precise Point Positioning (PPP) technique, through a long measurement session. Coordinates are computed in the ITRF20-UTM zone 36 N reference system (epoch 2025.3). The expected positioning accuracy is within 2 cm in the horizontal component and within 5 cm in the vertical component [26].

Figure 2. The fixed reference GNSS antenna mounted on the electric cabin present on the site.

The georeferencing of the SLAM surveys was then achieved in two different ways. For surveys conducted entirely in open spaces, an integrated Real-Time Kinematic (RTK) GNSS module was mounted on the mobile mapping system, with a declared relative positioning accuracy of ± 2 cm [27]. Instead, for the survey of hypogeal structures, georeferencing is obtained by including in the SLAM survey a few ground control points measured by a rover station in the surrounding area using a static-rapid technique.

This strategy was selected both for scientific and operational reasons. From a methodological standpoint, embedding absolute positioning constraints within the SLAM optimization process improves trajectory stability and limits long-term drift, particularly in extended surveys that combine open areas with GNSS-denied underground segments. From a practical perspective, the integrated GNSS approach allows rapid deployment and continuous acquisition without interrupting fieldwork for external control measurements, which is critical in time-constrained archaeological missions and harsh environmental conditions.

2.3. SLAM Mobile Laser Scanning Acquisition

The core of the survey methodology involved both handheld (for interiors) and backpack-mounted (for landscape mapping) mobile laser scanning based on the SLAM device Stonex X120GO, (Figure 3a). The scanner model employed provides dense 3D data with a declared relative accuracy of up to 6 mm and an operational scan range between 0.5 m and 120 m, as specified by the manufacturer [28].

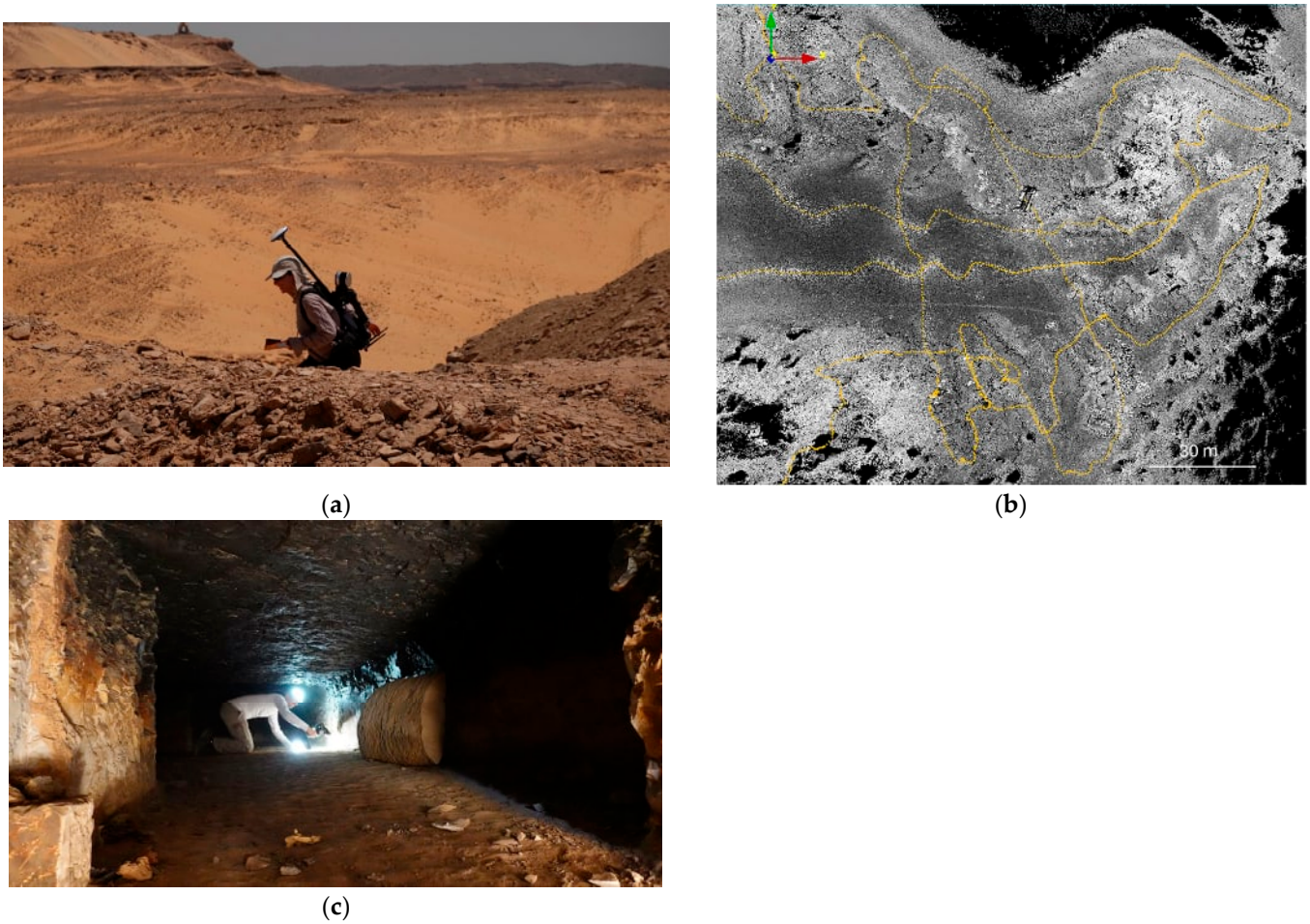

(**a**) (**b**)

(**c**)

Figure 3. Field acquisition phase: (**a**) The backpack configuration of the SLAM-GNSS receiver system; (**b**) An example of acquisition trajectory for SLAM surveying—the orange dots represent the path of the operator while scanning; (**c**) Operating the SLAM inside a tomb. The limited height of the hypogeal spaces (in the case of this figure, about 0.6 m) prevented the operator from standing upright in most areas, except for the stairways leading to the tomb entrances and for a few small sections where it was possible to stand, though only while bending.

The data acquisition was conducted during two field campaigns in 2023 and 2025, through multiple traverses covering all the recent excavation area, the surrounding territory, and the interiors of hypogeal tombs, including narrow corridors and secondary chambers. The survey activities were distributed between the two campaigns because the geomatic operations were constrained to short field missions lasting only a few days, which did not allow the complete coverage of the necropolis in a single campaign. Moreover, archaeological excavations are still ongoing and progressively uncover new areas and tombs; therefore, the SLAM documentation proceeded in parallel with the advancement of the archaeological work, extending the mapped areas during subsequent missions.

Each SLAM trajectory was designed in advance based on satellite imagery and preliminary site maps, enabling an initial assessment of the spatial extent of the necropolis and the identification of feasible walking paths for the operators. The survey planning was further refined on site through close collaboration with the archaeologists, prioritizing areas of particular interest while ensuring progressive coverage of the broader territory. Individual acquisition trajectories averaged approximately 20 min, ranging from about 10 min for short scans within individual tombs to 30–33 min for longer paths across more extensive open areas (up to 300 m in length). The SLAM device was powered by interchangeable batteries; two sets of batteries were used during each surveying day to ensure operational

continuity, as a single one allowed approximately four to five acquisition runs (roughly two hours of active scanning).

Particular attention was devoted to the definition of the acquisition trajectories. Rather than relying on single linear traverses, the survey strategy incorporated multiple passes and transversal overlaps, with operators repeatedly covering the same areas along intersecting paths. These trajectories often followed cross-shaped or S-shaped patterns, producing loop closures and redundant observations that strengthened the internal consistency of the SLAM solution and improved the overall spatial completeness of the reconstructed point clouds (Figure 3b).

Acquisition was performed under field conditions with limited time (5–6 h from early morning to 12 a.m.–1 p.m.), poor lighting in subterranean environments (Figure 3c), and the absence of a GNSS signal inside the tombs. The active LiDAR sensor enabled continuous mapping independent of ambient illumination, capturing millions of 3D points per scanning session (nominally, 320,000 points per second) as operators moved through the site. In addition, a set of three cameras is integrated in the scanning device to obtain panoramic images that are used in post-processing to texturize the point cloud.

2.4. SLAM Data Processing Workflow

After field acquisition, the raw SLAM datasets were processed using the proprietary GOpost software environment (v76), following a structured multi-stage workflow designed to ensure both global georeferencing accuracy and internal geometric consistency. For surveys conducted with the integrated RTK module, the GNSS data were first processed in post-processing kinematic (PPK) mode due to the absence of a real-time network connection between the module and the master station receiver. The expected accuracy of PPK mode is in the order of a few centimetres. Secondly, GOpost software computed the SLAM solution using LiDAR-based odometry and inertial data only, generating an initial point cloud in a local instrumental coordinate system. The GNSS trajectory is then used for the orientation and georeferencing in a global reference frame (UTM-ITRF2020) through a non-rigid coordinate transformation (Figure 4a). This procedure also helps to compensate for accumulated odometric drift and ensure global consistency.

Finally, RGB data acquired by the integrated cameras (Figure 4b) were projected onto the LiDAR-derived geometry to generate textured point clouds. Regarding the processing time, the duration was influenced by both the workstations employed and the scanning session length. While some datasets (e.g., tomb interiors) contained tens of millions of points, others covering large open areas reached hundreds of millions. Using high-performance workstations equipped with 256–512 GB of RAM, 7th- or 9th-generation multi-core CPUs, and advanced GPUs, the total processing time—including both automated computation and operator intervention—was on the order of several hours per dataset.

The resulting point clouds were then subjected to systematic cleaning and filtering procedures, including statistical outlier removal and manual removal of unwanted features captured in the point clouds, such as vehicles or people moving around the site. After this phase, the comprehensive point cloud was used to produce georeferenced DSMs, as well as sections and plans of the tombs' geometry.

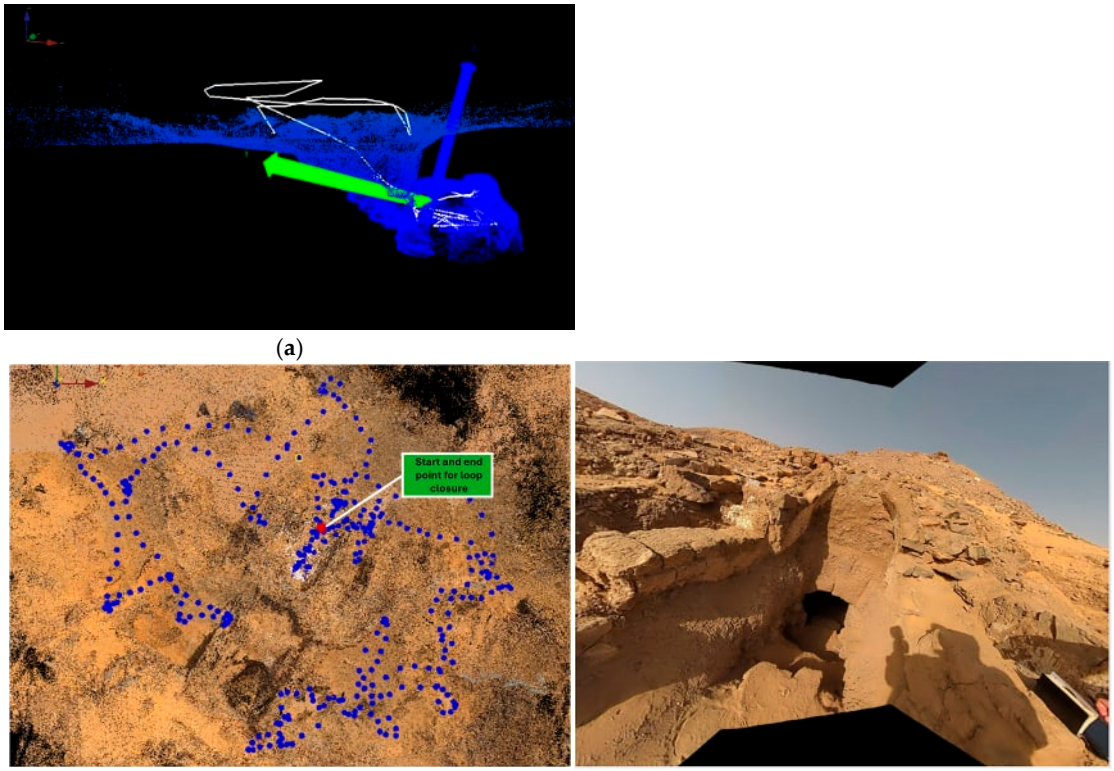

(**a**)

(**b**) (**c**)

Figure 4. (**a**) Initial processing phase of simultaneous trajectory estimation and cloud computation for an above- below-ground transition; the white line represents the scanning trajectory, with the X,Y,Z axes showing the instrument's orientation (**b**) SLAM odometry visualized (blue dots) on the cloud showing the loop-closed trajectory; (**c**) Portion of a panoramic image (undistorted) captured by the scanner-embedded cameras to texturize the point cloud.

2.5. Internal Coherency Evaluation of the Obtained Point Clouds

The multi-session SLAM survey conducted in 2023 and 2025 produced a set of point clouds (18 in total) acquired across various portions of the archaeological area, including five complete hypogeal tombs and several unexcavated tombs' entrances. The reciprocal alignment of this dataset was ensured through consistent georeferencing of all point clouds to the same cartographic reference system. Nevertheless, an additional assessment of their internal coherence was performed using Cloud-to-Cloud (C2C) analysis.

This analysis was carried out using the open-source software CloudCompare (v2.14) [29] for point-cloud processing. First, pairs of point clouds were selected based on their spatial overlap, selecting those with the highest mutual coverage. Each selected pair was then subjected to C2C distance computation, which estimates, for each point in one cloud, the closest corresponding point in the other dataset and calculates the resulting 3D distances. The obtained RMSE (Root Mean Square Error) values and standard deviations were subsequently summarised in tables and graphs for analytical evaluation of the results (Section 3.2). In addition, the entire procedure was repeated after an ICP (Iterative Closest Point) refinement step to assess whether the registration improved the dataset's internal coherence.

3. Results

3.1. Outcomes of the Integrated Above–Below-Ground 3D Reconstruction

The integrated survey approach, combining SLAM acquisitions with satellite-based positioning, produced a comprehensive georeferenced 3D reconstruction of both the above-

ground landscape and the subterranean hypogeal structures of the necropolis. Regarding the georeferencing procedure, the resulting point clouds achieve a differential positioning accuracy of approximately 2 cm, as declared by the manufacturer and validated through internal consistency analyses (described in Section 2.5). This workflow enabled efficient, continuous spatial documentation and georeferencing of both surface and hypogeal structures, while maintaining the geometric coherence required for archaeological interpretation and multi-temporal integration. The SLAM survey generated a dense, high-resolution point cloud covering approximately an area of 0.077 km^2, comprising more than 1 billion points. More specifically, the final point cloud consisted of approximately 1.04×10^9 points distributed over the mentioned area, resulting from 18 point clouds, 7 obtained in the 2023 campaign and 11 in 2025. The resulting point density ρ was computed as $\rho = \frac{N}{A}$ (where N is the total number of points and A is the 3D area). This calculation translates to an average density of 11,400 points per square meter. Assuming a quasi-uniform spatial distribution, the corresponding mean point spacing (spatial resolution) was estimated as $d \approx \sqrt{\frac{1}{\rho}}$ (where ρ is the calculated density), resulting in an average inter-point distance d of approximately 1 cm. Hence, rapid mobile mapping enabled the acquisition of extensive areas at centimetric-level densities that would otherwise require several days of static measurements (Figure 5).

Figure 5. The final point cloud visualized with RGB colours (scale bar unit is meters).

The merged SLAM datasets collected over the two survey campaigns were used to produce a 3D dataset capable of revealing morphological and slope variations—especially when shaders were applied to emphasize the geometry—and the spatial distribution of tomb entrances across the landscape (Figure 6). A corresponding DSM instead provided an overview of elevation and slope throughout the site (Figure 7).

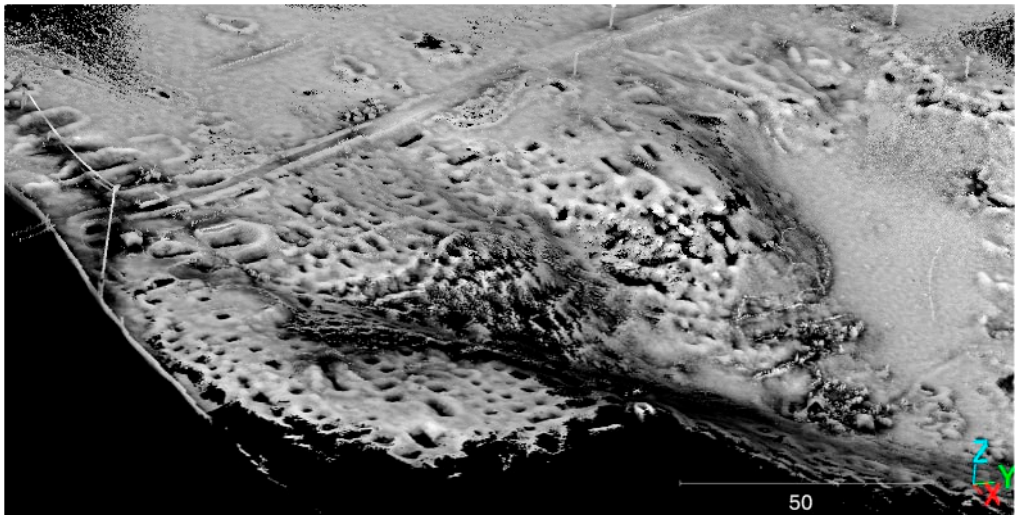

Figure 6. A view of the point cloud visualized with PCV (Portion de Ciel Visible) shader, highlighting the position of several tombs' entrances (scale bar unit is meters).

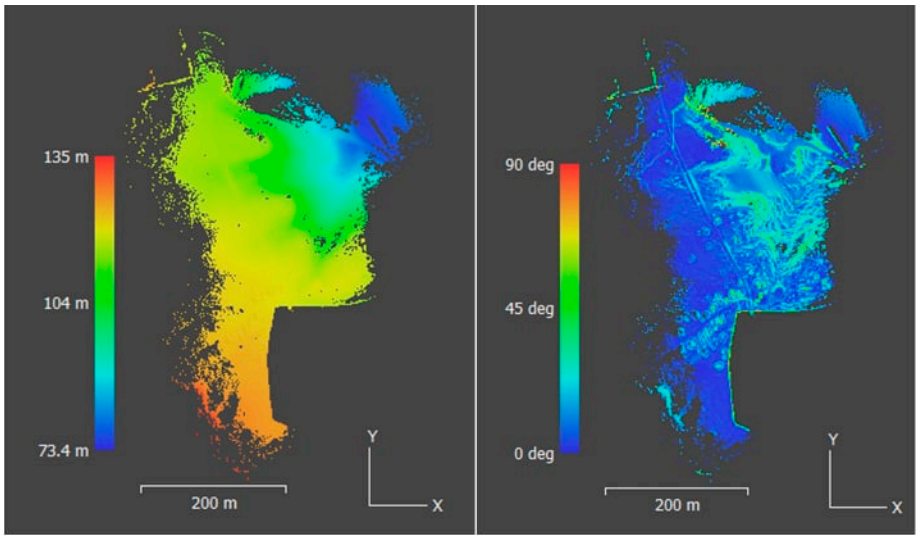

(**a**) (**b**)

Figure 7. The extracted DSM visualized with the palette showing elevation (**a**) and slope (**b**).

Finally, the fusion with satellite imagery—employed to produce a very high-resolution panchromatic georeferenced orthophoto—permitted us to situate the SLAM point cloud and the necropolis in its environmental and geomorphological context (Figure 8).

The integration of above-ground and below-ground datasets resulted in a seamless and georeferenced 3D model, enabling a continuous representation of both the terrain and the interior geometry of the hypogeal structures (Figure 9). The survey of multiple tombs interiors, some of which include narrow corridors, multi-room chambers, and complex vertical relationships with the ground surface, allowed to document and inspect the architectural morphology of these complex underground structures (Figure 10), calculating also their internal volume and area (for instance, the area of the tomb in the Figure is around 39 square metres).

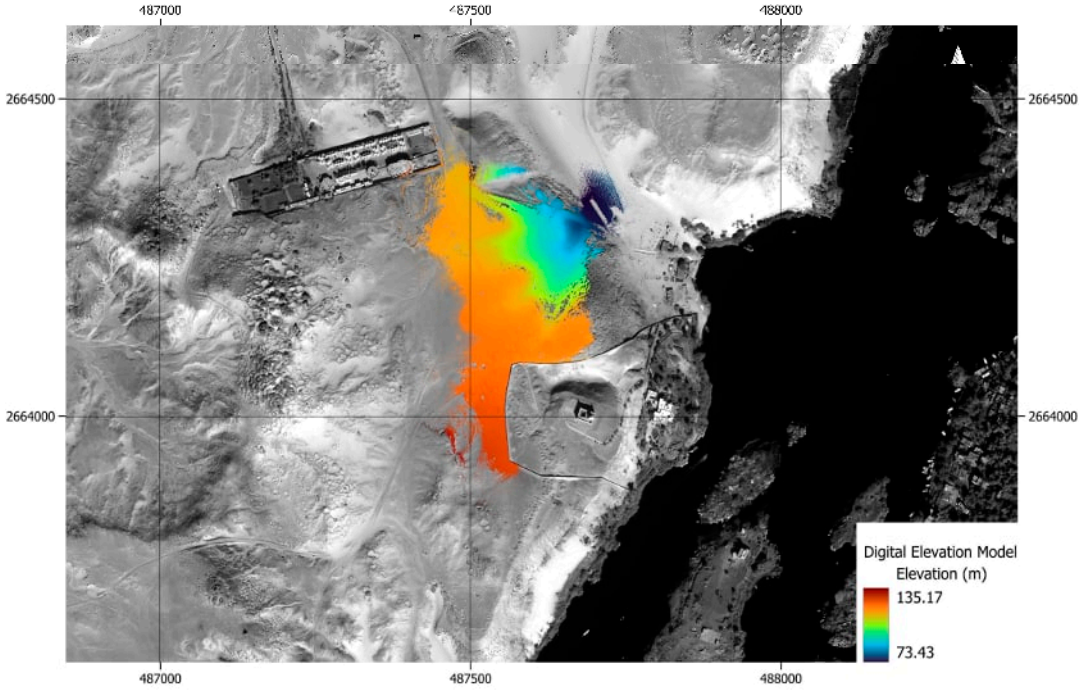

Figure 8. The DSM obtained from the point cloud visualized in GIS alongside the satellite imagery-derived orthophoto.

Figure 9. A view of a portion of the point cloud showing simultaneously the above- and below-ground reconstructed surface for the tomb AGH032 (scale bar unit is meters).

The SLAM-based LiDAR system proved particularly effective underground: unlike classical photogrammetry, which would have required extensive artificial and consistent illumination, the active sensor performed reliably in low-light conditions (the sole illumination source was the sunlight coming from the tombs' opening and some portable light devices). The 3D geometric models also supported the production of graphical products, including sections and plans, for documenting the internal organisation of these hypogeal structures (Figure 11).

Figure 10. Top view of a portion of the point could for the tomb AGH032 showing both above and below-ground surface in "X-Ray" mode.

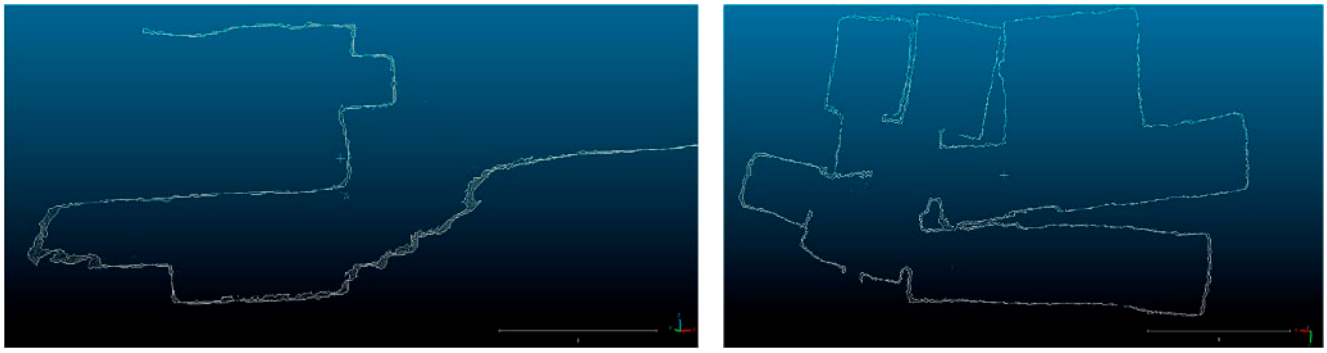

(**a**) (**b**)

Figure 11. (**a**) Transversal section of tomb AGH032 entrance and its internal structure; (**b**) Generated plan of the same tomb, showing the multiple ambiences configuration (scale bar unit is in meters).

Overall, the integrated approach enabled a multiscale, continuous, and metrically accurate 3D representation of the necropolis, significantly improving both documentation and spatial analysis capabilities.

3.2. Internal Coherency Evaluation Results

The Cloud-to-Cloud (C2C) analysis provided a quantitative assessment of the internal coherence of the multi-session SLAM dataset, acquired over two campaigns. The objective of this evaluation was to verify whether the georeferencing strategy based on integrated RTK-SLAM trajectory correction was sufficient to ensure reciprocal alignment among independently acquired point clouds and to quantify the additional benefit introduced by ICP-based refinement.

The pre-ICP comparisons already demonstrate a good level of internal consistency across the dataset. For the 2023 acquisitions, mean C2C distances ranged approximately between 0.010 and 0.025 m, with an overall average of 0.016 m and a negligible standard deviation of 0.006 m. These results indicate centimetric agreement between overlapping clouds acquired in separate sessions, confirming the effectiveness of the RTK-aided SLAM georeferencing and trajectory correction workflow in controlling both global positioning error and cumulative SLAM drift. Such deviations remain compatible with the accuracy requirements for the archaeological documentation and spatial analysis demanded for this work. Post-ICP results for 2023 clouds show a redistribution of the C2C distances among individual cloud pairs, with local improvements observed in most comparisons, while the overall mean and standard deviation remain unchanged (Table 1, Figure 12). This behaviour could indicate that the ICP refinement acted primarily as a local geometric adjustment rather than as a global alignment correction, consistent with the fact that GNSS observations were already integrated within the SLAM backend. Notably, one cloud pair exhibits a slightly higher mean C2C distance after ICP; this effect could be attributed to local geometric conditions, such as reduced overlap or weaker geometric constraints, and does not reflect a degradation of the global alignment. Figure 13 displays visually the C2C results for the case described above.

Table 1. Results of the C2C procedure for the 2023 dataset (pre- and post-ICP comparison).

2023 C2C Results	Average Value (m)	Average Value (m)
Cloud pair	PRE-ICP	POST-ICP
1	0.009	0.009
2	0.025	0.021
3	0.012 (visual results in Figure 12)	0.019
4	0.016	0.014
	Average all pairs 2023 = 0.016	
	St.Dev. all pairs 2023 = 0.006	

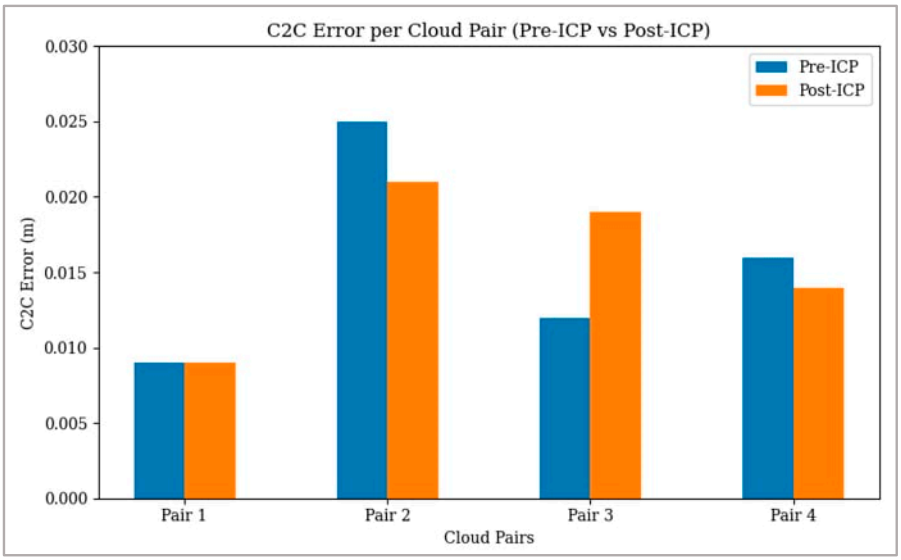

Figure 12. Graphical representation of C2C results for the 2023 dataset (pre- and post-ICP comparison).

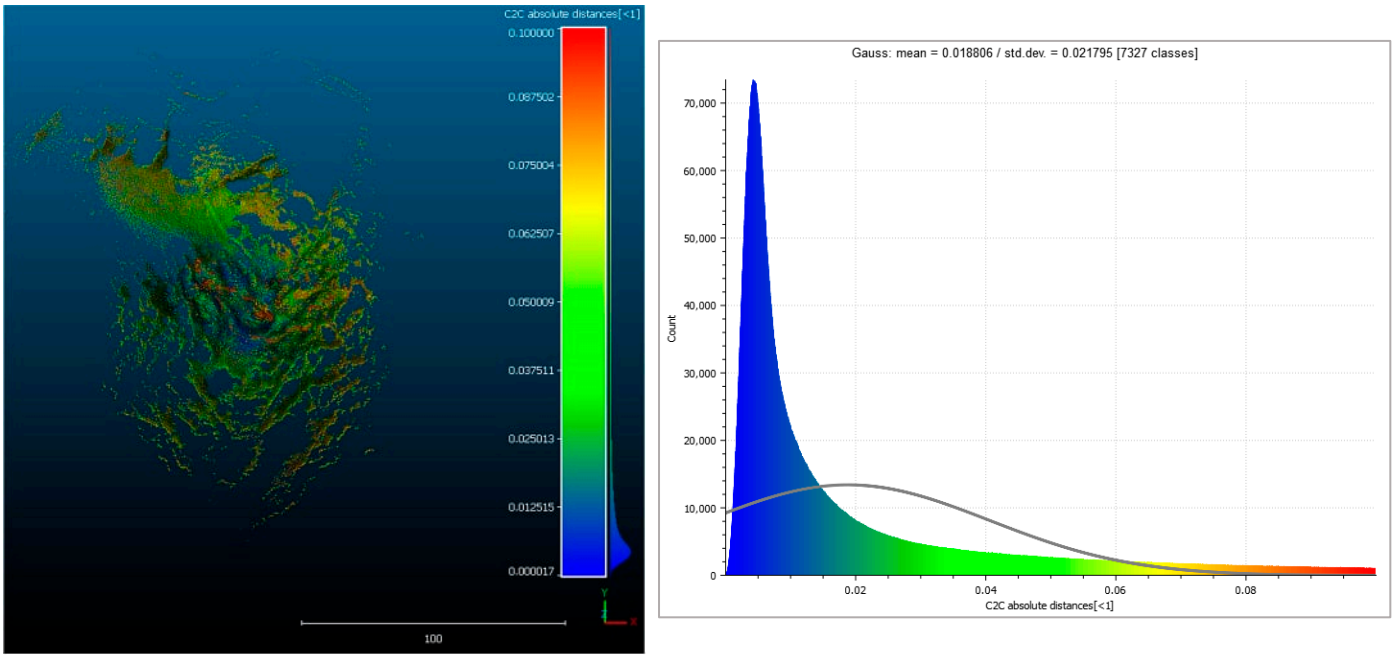

(**a**) (**b**)

Figure 13. (**a**) Visual representation of the C2C result (post-ICP) for pair 3 (2023 dataset), showing the distance values (meters) with colour gradient (scale bar unit is meters); (**b**) histogram of the C2C distance values, gaussian fitting.

The 2025 dataset exhibits slightly higher variability, with mean C2C distances ranging from approximately 0.021 to 0.047 m and an overall mean of 0.030 m (standard deviation 0.009 m, Table 2). This increased dispersion can be attributed to a combination of factors, including longer trajectories, greater geometric homogeneity in the topography of some areas, and, more generally, a higher number of individual clouds and acquired points (11 clouds for a total point count of over 630 million). A visual representation of the C2C results for a representative cloud pair is shown in Figure 14. The example refers to two SLAM acquisitions characterized by long predominantly linear trajectories, exceeding 300 m in length. The spatial distribution of the C2C distances highlights a progressive increase in discrepancies along the trajectory, with the highest deviations occurring toward the terminal portion of the path. This pattern clearly reflects the cumulative nature of procedural drift in SLAM-based mapping, which becomes more pronounced as the trajectory length increases, particularly in extended and weakly constrained linear environments. As a result, centimetric-level geometric discrepancies may arise in the reconstructed point clouds, becoming evident when independently acquired datasets following similar paths are compared.

Table 2. Results of the C2C procedure for the 2025 dataset (pre- and post-ICP comparison).

2025 C2C Results	**Average Value (m)**	
Cloud pair	PRE-ICP	POST-ICP
1	0.024	0.022
2	0.047 (visual results in Figure 14)	0.045
3	0.029	0.028
4	0.035	0.032
5	0.024	0.023
6	0.022	0.022
	Average 2025 = 0.030 St.Dev. 2025 = 0.009	

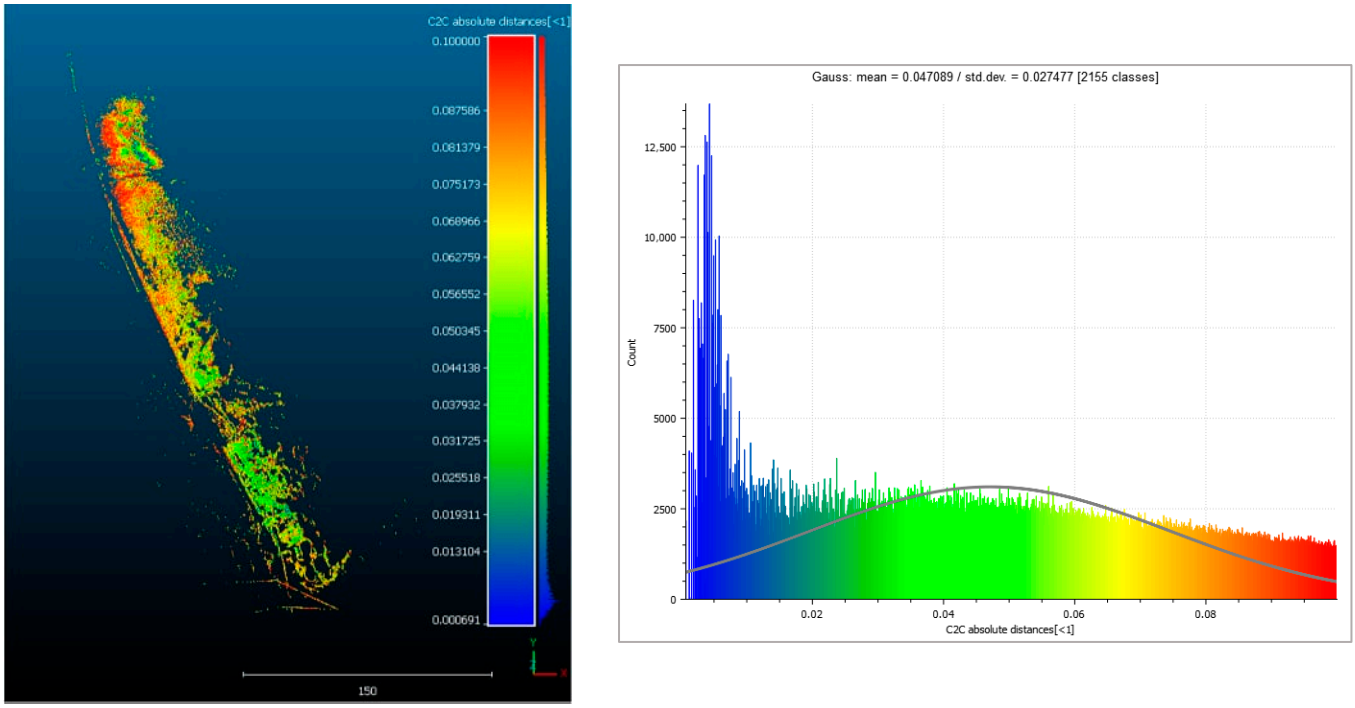

(**a**) (**b**)

Figure 14. (**a**) Visual representation of the C2C result for pair 2 (2025 dataset, worst result) showing the distance values (meters) with colour gradient (scale bar unit is meters); (**b**) histogram of the C2C distance values, gaussian fitting.

Nonetheless, even in this second survey campaign, most pairwise comparisons remained within a few centimetres, indicating that the adopted georeferencing strategy maintained an acceptable level of coherence—compliant with the survey objectives—across temporally separated datasets covering a large-scale site. For the 2025 dataset, post-ICP results exhibit trends consistent with those observed for the 2023 acquisitions, confirming that the alignment refinement produced only negligible millimetric-level improvements, generally limited to sub-centimetric magnitudes. This behaviour suggests that the initial alignment achieved through RTK-assisted SLAM processing already provided a few-centimetric level of reciprocal cloud consistency, leaving limited scope for further correction through registration algorithms. In this context, ICP primarily acted as a fine-tuning procedure, redistributing residual discrepancies rather than compensating for significant systematic misalignments.

Overall, the Cloud-to-Cloud analysis demonstrates that the SLAM georeferencing strategy, based on integrated RTK observations and inertial trajectory correction, provides a robust, metrically consistent framework for multi-session data integration. Across different acquisition campaigns and survey conditions, the resulting point clouds exhibit stable centimetric-level internal coherence, confirming that SLAM-derived trajectory estimation is the primary determinant of geometric accuracy. The limited impact of ICP refinement on the global statistics further indicates that the dataset quality is largely established during the SLAM processing stage, where GNSS and inertial measurements are coherently integrated into the backend optimization. In this context, ICP operates mainly as a local fine-tuning mechanism, redistributing residual discrepancies without compensating for significant systematic misalignments, and thus does not fundamentally alter the geometric quality of the reconstruction. This behaviour is consistent across both survey campaigns and highlights the effectiveness of the adopted RTK-assisted SLAM workflow in controlling cumulative drift over extended trajectories and temporally separated acquisitions.

It should be emphasized that the reported C2C validation applies exclusively to the external survey areas, where partial overlap between independent acquisitions enables quantitative inter-cloud comparisons. Conversely, the hypogeal environments, including the individual tombs, were documented as standalone datasets, each represented by a single point cloud with no internal overlap. Consequently, a C2C-based assessment of internal coherence was not applicable to these portions of the dataset, whose geometric reliability relies instead on the intrinsic consistency of the SLAM reconstruction and the integrated trajectory estimation. Nevertheless, the hypogeal spaces are characterized by limited spatial extent and high architectural complexity, providing strong geometric constraints on SLAM-based mapping. Unlike elongated underground environments such as tunnels or galleries, which are typically characterized by linear, repetitive geometries, the compact, articulated morphology of the tombs inherently enhances SLAM stability and mitigates drift accumulation.

4. Discussion

4.1. Discussion of Outcomes in the Context of Related Literature

The results presented in this article confirm the distinctive added value of SLAM-based mobile mapping in archaeological contexts that combine extensive open areas with complex subterranean components, while also advancing the state of the art relative to previously published applications. Earlier studies demonstrated the SLAM effectiveness primarily in confined or exclusively underground environments [18,19]. Our work complements these findings by showing that SLAM can be successfully deployed not only in enclosed hypogeal spaces but also across a large desert necropolis, integrating broad exterior terrains, valley slopes, and multiple tombs into a single, continuous, georeferenced dataset—a scale and typological diversity not previously demonstrated in the literature. This constitutes a substantial methodological progression beyond studies that relied on combining separate TLS, UAV, and photogrammetric datasets to achieve above–below-ground integration [6,7]. In contrast, the approach in EIMAWA shows that a SLAM-based workflow, when coupled with proper geodetic positioning, can produce an integrated and coherent multi-scale model of an entire and complex archaeological landscape.

4.2. Advantages and Limitations of SLAM in Complex Archaeological Contexts

Within this framework, SLAM proved particularly advantageous due to its speed and continuity in acquiring spatial data across diverse environmental conditions. Extensive exterior areas and the interiors of numerous tombs were documented in a seamless workflow, avoiding the segmented acquisition and station planning required by TLS or total-station methods. This efficiency is particularly meaningful in harsh desert settings, where rapid changes in daylight, heat exposure, and uneven terrain can constrain the feasibility of slower, static surveys. The ability of LiDAR-based SLAM to operate independently of ambient illumination further enabled direct transitions between bright, open-air sectors and unlit chambers without modifying the acquisition configuration. This continuity is not simply a practical benefit: it allows the creation of a spatially coherent, above–below-ground model in which relationships among terrain morphology, entrances, and internal tomb architecture can be examined jointly, without the discontinuities that typically arise when integrating disparate sensor technologies.

A second major outcome concerns the global geodetic consistency of the resulting dataset. By integrating GNSS observations directly into the SLAM backend together with inertial measurements, a few-centimetric-level globally consistent model was achieved, allowing the point cloud to be recomputed directly within the ITRF/UTM reference frame. This approach highlights the relevance of absolute positioning in SLAM-based archae-

ological applications, where datasets are often confined to local coordinate systems or georeferenced only through post hoc alignment to external references. The implemented workflow, therefore, demonstrates that a carefully planned SLAM pipeline can meet not only the continuity and efficiency requirements imposed by complex archaeological environments, but also the level of geometric rigour necessary for excavation planning and spatial analysis.

Nonetheless, the experience described in this article also aligns with the limitations identified in previous studies. Drift remains an inherent issue, especially over long or feature-poor outdoor trajectories, making loop closures and repeated traverses essential. In addition, it should be considered that the GNSS trajectory is introduced after the local SLAM reconstruction, serving primarily as a geodetic orientation constraint on a geometry already reconstructed in a local reference frame. As a consequence, while GNSS integration effectively anchors the dataset to an absolute coordinate system and mitigates global drift, it cannot fully compensate for locally accumulated errors arising during the incremental mapping process. Moreover, operator motion and speed, trajectory curvature and length, as well as coverage strategies and inter-scan overlap, directly influence data completeness, noise distribution, and local geometric stability. These factors highlight that SLAM-based surveying is not a fully automatic process but rather requires specialized operator training and carefully planned acquisition strategies. This aspect becomes particularly critical in subterranean environments such as tomb corridors and chambers. Based on the experience gained during the described surveys, practical considerations emerged for the acquisition of SLAM datasets in hypogeal contexts. In particular, it is advisable to prioritize relatively short trajectories with a loop-closure design, starting outside the tomb and then. after scanning the interior. coming back to the same point outside again. Equally important is the control of operator motion: slow, controlled movements, especially when descending into tomb entrances or moving along steep access paths, are essential to avoid abrupt accelerations that may challenge the scanner's IMU and potentially compromise feature tracking.

These recommendations are closely related to the intrinsic constraints of underground environments. Hypogeal archaeological spaces often consist of narrow passages, steep descending corridors, abrupt elevation changes, and geometrically complex access routes that can make operator movement unstable and limit the availability of distinctive spatial features for the SLAM algorithm. In addition, the absence of natural light reduces the operator's ability to perceive the broader spatial configuration of the environment, making trajectory control more difficult during acquisition. In such conditions, slow and controlled movement, and redundant coverage of the same areas through loop closures and multi-pass scanning, become useful operational strategies to mitigate drift, maintain tracking stability, and ensure the geometric completeness of the resulting point clouds.

Post-processing also proved demanding, requiring time-consuming operations such as map orientation and generation, loop-closure refinement, manual point cloud cleaning, and cloud-to-cloud evaluation to ensure the final dataset was geometrically consistent and suitable for analysis. These steps reinforce the notion that SLAM, despite its evident efficiency during field acquisition, is not a "plug-and-play" replacement for traditional surveying methods, but rather a technique that shifts part of the operational complexity from the field to the processing stage.

Finally, while point cloud density was generally sufficient for the spatial and morphological analyses within the scope of this work, SLAM does not achieve the higher accuracy of survey-grade TLS, making it less suited for applications requiring fine architectural diagnostics or deformation monitoring.

5. Conclusions

In conclusion, the work carried out at West Aswan demonstrates the effectiveness of an integrated geomatic strategy centred on SLAM mobile laser scanning and supported by GNSS georeferencing. This approach enabled the creation of a coherent, multi-scale, and fully georeferenced 3D archive of the necropolis, capable of representing both the extensive desert landscape and the intricate architecture of its hypogeal tombs. The capacity of SLAM to function efficiently under harsh environmental conditions and in unlit subterranean spaces was crucial to achieve comprehensive documentation within the mission logistical constraints, providing a level of spatial continuity that would have been difficult to obtain through static or aerial methods alone. Although SLAM cannot yet match the millimetric accuracy of survey-grade TLS, its portability, speed, and illumination independence make it an essential component of archaeological documentation workflows in complex and evolving field contexts. A quantitative assessment of the absolute positioning accuracy and geometric reliability of the SLAM datasets was beyond the scope of the present work and therefore represents a current open issue of the study. Future survey campaigns will aim to address this aspect by establishing an external topographic or geodetic control network, or by comparing with independent ground-truth measurements acquired with TLS or Total Station (TS) techniques, when these are logistically available and operational conditions and survey time allow.

Beyond the immediate results, this work lays the spatial foundation for future documentation and interpretative studies of the necropolis. A key prospect could be the expansion of the current 3D archive into a comprehensive, multi-disciplinary geodatabase that integrates high-detail photogrammetric models, thereby combining SLAM-derived spatial continuity with the finer geometric and texture information derived from image-based reconstruction. Such a unified framework will also make it possible to incorporate other types of archaeological and scientific data—including discoveries from bioarchaeological, chemical, and Egyptological investigations—thereby creating a richer spatial platform for analysis, interpretation, and cross-disciplinary research. Within this framework, the integration of an external verification network and independent reference datasets would further strengthen the quantitative evaluation of SLAM reconstructions, enabling more rigorous validation of both positioning accuracy and geometric consistency in future missions. As excavations progress and new areas of the necropolis are uncovered, the integrated SLAM-GNSS pipeline can be extended to continuously update the geodatabase, supporting both diachronic documentation and the long-term management of the site. In this perspective, the work conducted so far represents not an endpoint, but the foundation for a dynamic and evolving digital record of this—and potentially other—archaeological sites.

Author Contributions: Conceptualization, G.B. and E.M.; methodology, G.B., A.F. and E.M.; validation, G.B., A.F. and E.M.; formal analysis, G.B. and E.M.; investigation, G.B. and A.F.; resources, G.B.; data curation, G.B., A.F. and E.M.; writing—original draft preparation, A.F.; writing—review and editing, G.B. and E.M.; visualization, A.F.; supervision, G.B. and E.M.; project administration, G.B. All authors have read and agreed to the published version of the manuscript.

Funding: This research received no external funding.

Informed Consent Statement: Informed consent was obtained from all subjects involved in the study.

Data Availability Statement: The datasets presented in this article are not readily available because the data are part of an ongoing study.

Acknowledgments: This activity has been carried out in the framework of the Egyptian–Italian Mission at West Aswan (EIMAWA) led by P. Piacentini from the University of Milano and Fahmy

el-Amin, seconded by A. Cavagna and M. Pozzi Battaglia. The authors wish to thank all of the components of the mission and A. Polito, who worked on the initial processing of the 2023 campaign data.

Conflicts of Interest: The authors declare no conflicts of interest.

Abbreviations

The following abbreviations are used in this manuscript:

C2C	Cloud-to-Cloud (distance)
CPU	Central Processing Unit
DEM	Digital Elevation Model
DTM	Digital Terrain Model
EIMAWA	Egyptian–Italian Mission at West-Aswan
GNSS	Global Navigation Satellite System
GPU	Graphics Processing Unit
GSD	Ground Sampling Distance
ICP	Iterative Closest Point
IMU	Inertial Measurement Unit
LiDAR	Light Detection and Ranging
MMS	Mobile Mapping System
PCV	Portion de Ciel Visible
RMSE	Root Mean Square (error)
RTK	Real-Time Kinematic
SfM	Structure-from-Motion
SLAM	Simultaneous Localization and Mapping
TLS	Terrestrial Laser Scanning
UAV	Unmanned Aerial Vehicle
UTM	Universal Transverse Mercator

References

1. Liang, H.; Li, W.; Lai, S.; Zhu, L.; Jiang, W.; Zhang, Q. The integration of terrestrial laser scanning and terrestrial and unmanned aerial vehicle digital photogrammetry for the documentation of Chinese classical gardens: A case study of Huanxiu Shanzhuang, Suzhou, China. *J. Cult. Herit.* **2018**, *33*, 222–230. [CrossRef]
2. Bitelli, G. Remote sensing and integration with other geomatic techniques in archaeology. In *Satellite Remote Sensing (Remote sensing and Digital Image Processing)*; Lasaponara, R., Masini, N., Eds.; Springer: Berlin/Heidelberg, Germany, 2012; Volume 16, pp. 87–110. [CrossRef]
3. Ulvi, A. Using UAV photogrammetric technique for monitoring, change detection, and analysis of archaeological excavation sites. *J. Comput. Cult. Herit.* **2022**, *15*, 43. [CrossRef]
4. Tini, M.A.; Forte, A.; Girelli, V.A.; Lambertini, A.; Roggio, D.S.; Bitelli, G.; Vittuari, L. Scan-to-HBIM-to-VR: An integrated approach for the documentation of an industrial archaeology building. *Remote Sens.* **2024**, *16*, 2859. [CrossRef]
5. Forte, A.; Alkhatib, Y.; Bitelli, G.; Malinverni, E.S.; Pierdicca, R. Geomatics and metaverse for lost heritage sites documentation and dissemination: The case study of Palmyra Roman Theatre (Syria). *Virtual Archaeol. Rev.* **2024**, *16*, 85–99. [CrossRef]
6. Ebolese, D.; Lo Brutto, M.; Dardanelli, G. The integrated 3D survey for underground archaeological environment: The Sybil hypogeum and overhead complex (Lilibeo, Italy). *Int. Arch. Photogramm. Remote Sens. Spat. Inf. Sci.* **2019**, *XLII-2/W9*, 311–318. [CrossRef]
7. Aricò, M.; La Guardia, M.; Lo Brutto, M. Web exploration of cultural heritage with limited accessibility: First experimentation for hypogeum archaeological sites. *Int. Arch. Photogramm. Remote Sens. Spat. Inf. Sci.* **2023**, *XLVIII-M-2*, 111–118. [CrossRef]
8. Chiabrando, F.; Sammartano, G.; Spanò, A.; Semeraro, G. Multi-temporal images and 3D dense models for archaeological site monitoring in Hierapolis of Phrygia (TK). *Archeol. Calc.* **2017**, *28*, 469–484. [CrossRef]
9. Alshawabkeh, Y.; Haala, N.; Fritsch, D. Integration of photogrammetry and laser scanning for enhancing scan-to-HBIM modeling of Al Ula heritage site. *npj Herit. Sci.* **2023**, *11*, 147. [CrossRef]
10. Trybała, P.; Kasza, D.; Wajs, J.; Remondino, F. Comparison of low-cost handheld LiDAR-based SLAM systems for mapping underground tunnels. *Int. Arch. Photogramm. Remote Sens. Spat. Inf. Sci.* **2023**, *XLVIII-1/W1*, 517–524. [CrossRef]

11. Filip, I.; Pyo, J.; Lee, M.; Joe, H. LiDAR SLAM with a wheel encoder in a featureless tunnel environment. *Electronics* **2023**, *12*, 1002. [CrossRef]
12. Durrant-Whyte, H.; Bailey, T. Simultaneous localization and mapping (SLAM): Part I. *IEEE Robot. Autom. Mag.* **2006**, *13*, 99–110. [CrossRef]
13. Torresani, A.; Rigon, S.; Farella, E.M.; Menna, F.; Remondino, F. Unveiling large-scale historical contents with V-SLAM and markerless mobile AR solutions. *Int. Arch. Photogramm. Remote Sens. Spat. Inf. Sci.* **2021**, *XLVI-M-1*, 761–768. [CrossRef]
14. Beltramone, L.; De Lucia, V.; Ermini, A.; Innocenti, M.; Silvestri, D.; Rindinella, A.; Ronchitelli, A.; Ricci, S.; Boschin, F.; Salvini, R. Applying SLAM-based LiDAR and UAS technologies to evaluate the rock slope stability of the Grotta Paglicci Paleolithic site (Italy). *GeoHazards* **2024**, *5*, 457–484. [CrossRef]
15. Ortiz-Coder, P.; Sánchez-Ríos, A. A self-assembly portable mobile mapping system for archaeological reconstruction based on VSLAM–photogrammetric algorithm. *Sensors* **2019**, *19*, 3952. [CrossRef]
16. Ortiz-Coder, P.; Sánchez-Ríos, A. An integrated solution for 3D heritage modeling based on videogrammetry and V-SLAM technology. *Remote Sens.* **2020**, *12*, 1529. [CrossRef]
17. Malinverni, E.S.; Pierdicca, R.; Bozzi, C.A.; Bartolucci, D. Evaluating a SLAM-based mobile mapping system: A methodological comparison for 3D heritage scene real-time reconstruction. In *Proceedings of the 2018 Metrology for Archaeology and Cultural Heritage (MetroArchaeo)*; IEEE: New York, NY, USA, 2018; pp. 265–270. [CrossRef]
18. D'Agostino, G.; Figuera, M.; Russo, G.; Galizia, M.; Militello, P.M. Integrated 3D survey for the documentation and visualization of a rock-cut underground built heritage: Hypogeum of Calaforno (Sicily). *Int. Arch. Photogramm. Remote Sens. Spat. Inf. Sci.* **2022**, *XLVI-2/W1*, 167–174. [CrossRef]
19. Grasso, N.; Dabove, P.; Piras, M. The Use of SLAM and UAV technology in geological field for monitoring: The case study of the Bossea Cave. *Int. Arch. Photogramm. Remote Sens. Spat. Inf. Sci.* **2023**, *XLVIII-2/W3*, 73–79. [CrossRef]
20. Ebadi, K.; Bernreiter, L.; Biggie, H.; Catt, G.; Chang, Y.; Chatterjee, A.; Denniston, C.E.; Deschênes, S.P.; Harlow, K.; Khattak, S.; et al. Present and future of SLAM in extreme underground environments. *arXiv* **2022**, arXiv:2208.01787. [CrossRef]
21. El-Alaily, A.; Zhang, K.; Mea, C.; Perfetti, L.; Remondino, F.; Fassi, F. Coupling V-SLAM and semantic segmentation for cultural heritage documentation. *Int. Arch. Photogramm. Remote Sens. Spat. Inf. Sci.* **2025**, *XLVIII-M-9*, 435–442. [CrossRef]
22. Vega-Torres, M.A.; Braun, A.; Borrmann, A. SLAM2REF: Advancing long-term mapping with 3D LiDAR and reference map integration for precise 6-DoF trajectory estimation and map extension. *Constr. Robot.* **2024**, *8*, 13. [CrossRef]
23. Feng, C.; Yu, J.; Li, J.; Wang, K.; Wang, B.; Wu, Y. Evaluation of LiDAR SLAM algorithms for construction robots in large public construction sites. *Low-Carbon Mater. Green Constr.* **2025**, *3*, 28. [CrossRef]
24. Piacentini, P.; Pozzi, M. A multidisciplinary mission for Aga Khan Necropolis: The Egyptian Italian Mission at West Aswan (EIMAWA). In *Mathematical Modeling in Cultural Heritage*; Springer INdAM Series; Bretti, G., Cavaterra, C., Solci, M., Spagnuolo, M., Eds.; Springer: Berlin/Heidelberg, Germany, 2025; Volume 65. [CrossRef]
25. Piacentini, P. Assouan, VIe siècle av. J.-C.-IIe siècle ap. J.-C.: La découverte récente d'une nécropole de frontière. *Compte Rendus Séances L'acad. Inscr. Belles-Lett.* 2025, *in press*.
26. Cappuccio, M.; Tavasci, L.; Poluzzi, L.; Gandolfi, S. Study on the accuracy of multi-GNSS PPP for different observing session time spans using PRIDE PPP-AR open-source software package. *Appl. Geomat.* **2026**, *18*, 24. [CrossRef]
27. Stonex. S900+ GNSS Receiver. 2026. Available online: https://stonex.it/product/s900-plus-gnss-receiver/ (accessed on 10 January 2026).
28. Stonex. X120GO SLAM Laser Scanner. 2026. Available online: https://stonex.it/new-products/x120go-slam-laser-scanner/ (accessed on 10 January 2026).
29. Girardeau-Montaut, D. CloudCompare. *Fr. EDF R&D Telecom ParisTech* **2016**, *11*, 2016.